Design, Synthesis, Evaluation, and Crystallographic-Based Structural Studies of HIV-1 Protease Inhibitors with Reduced Response to the V82A Mutation[§]

José C. Clemente,[†] Arthur Robbins,[†] Paula Graña,[‡] M. Rita Paleo,[‡] Juan F. Correa,[‡] M. Carmen Villaverde,[‡] F. Javier Sardina,[‡] Lakshmanan Govindasamy,[†] Mavis Agbandje-McKenna,[†] Robert McKenna,[†] Ben M. Dunn,[†] and Fredy Sussman*[,‡]

Departamento de Química Orgánica, Facultad de Química, Universidad de Santiago de Compostela, 15782-Santiago de Compostela, Spain, and Department of Biochemistry and Molecular Biology, University of Florida College of Medicine, Gainesville, Florida 32610

Received September 18, 2007

In our quest for HIV-1 protease inhibitors that are not affected by the V82A resistance mutation, we have synthesized and tested a second generation set of C_2-symmetric HIV-1 protease inhibitors that contain a cyclohexane group at P1 and/or P1′. The binding affinity results indicate that these compounds have an improved response to the appearance of the V82A mutation than the parent compound. The X-ray structure of one of these compounds with the V82A HIV-1 PR variant provides the structural rationale for the better resistance profile of these compounds. Moreover, scrutiny of the X-ray structure suggests that the ring of the Cha side chain might be in a boat rather than in the chair conformation, a result supported by molecular dynamics simulations.

Introduction

Many research laboratories have developed HIV-1 protease (HIV-1 PR) inhibitors that have become lead compounds for antiviral drugs, and some of these compounds have been approved for therapeutical use.[1–4] It has been found that the most effective drug treatment, referred to as highly active antiretroviral therapy or HAART[a], is based on drug combinations, such as HIV-1 PR inhibitors and HIV-1 reverse transcriptase inhibitors.[5] Still, one of the pervading problems found in these therapies is the development of resistance mutations in the protease. During therapy with antiretroviral drugs, the pretherapy forms of the virus are inhibited from replication, while variant forms, created by the activity of the error-prone reverse transcriptase, are allowed to propagate. The primary sequence modifications that are encoded in this way are called "resistance" mutations and have been observed both in vitro and in vivo.[3–6] These sequence changes occur in a variety of residues located in the binding site as well as on the surface of the enzyme. The resistance mutations keep or enhance the catalytic activity of the enzyme, allowing the virus to replicate, but they lower the affinity of the HIV-1 PR for the antiviral drug, thus reducing its potential therapeutic power. One of the residues that is consistently mutated as a consequence of the HAART treatment, especially with Indinavir and Ritonavir,[7] is V82, which can be replaced by a variety of amino acids ranging from Ala to Phe. The V82A variant has been identified as a resistant mutant in vitro[5] as well as in clinical isolates.[4,6] X-ray crystallographic studies of a C_2 symmetric inhibitor bound to the V82A HIV-1 PR variant indicate that the V82A mutant breaks down the almost symmetric binding modes to the S1 and S1′ sites by reducing the interaction of the enzyme only with the P1 fragment.[8] This can be considered as a "hydrophobic defect" in the packing of the inhibitor−enzyme complex, similar to that produced by mutations in the core of the protein.[9] The design of a second generation C_2 pseudosymmetric inhibitors that are less affected by the V82A mutation could include more bulky groups in P1 or P1′ that could "repair" the above-mentioned "hydrophobic hole". To probe this hypothesis, we have synthesized and tested the known inhibitor **PP** (A-76928), a C_2-pseudosymmetric inhibitor with a diol motif based isostere,[10] as well as the related inhibitors **PC** and **CC** that replace one or two phenyl groups, respectively, by the larger cyclohexane fragment in this inhibitor (see Table 1). Our second generation inhibitors have a better resistance profile for the V82A mutations, demonstrating the validity of our design hypothesis.

X-ray-based structural studies (combined with a variety of other techniques) have afforded many insights into the mechanisms of resistance mutations, which have been used to produce and test second generation inhibitors or to design totally new inhibitors with improved resistance profile against a variety of

Table 1. Inhibitors Studied in this Work

Inhibitor[a]	Chemical Structure
PP	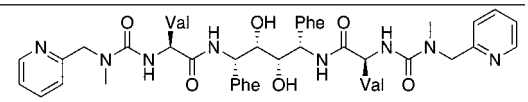
PC	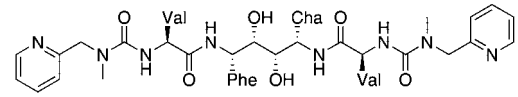
CC	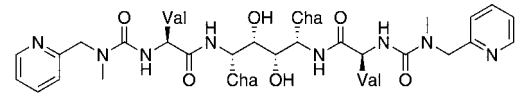
CGP 53820[b]	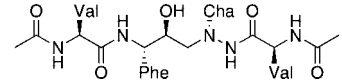

[a] The names **PP**, **PC**, and **CC** came from the P1/P1′ fragments, where P stands for Phe, the phenylalanine side chain, and C for Cha, the cyclohexylalanine side chain. [b] See ref 25.

[§] Coordinates for HIV-1 PR^{V82A} complexed with inhibitor **PC** (**9**) have been deposited in the Protein Data Bank, with access code 2FLE.

* To whom correspondence should be addressed. Phone: 0034981563100, ext 14402. Fax: 0034981591014. E-mail: fsussman@usc.es.

[†] University of Florida.

[‡] Universidad de Santiago de Compostela.

[a] Abbreviations: HAART, highly active antiretroviral therapy; Cha, cyclohexylalanine side chain; Cy, cyclohexyl; Cby, 2,2,4,4-tetramethyl-1,3-oxazolidine-3-carbonyl; IPTG, isopropylthio-D-galactopyranoside; dTT, dithiothreitol.

10.1021/jm701170f CCC: $40.75
Published on Web 01/24/2008

Scheme 1. Total synthesis of HIV-1 protease inhibitors **CC** (**8**), **PC** (**9**), and **PP** (**10**)[a]

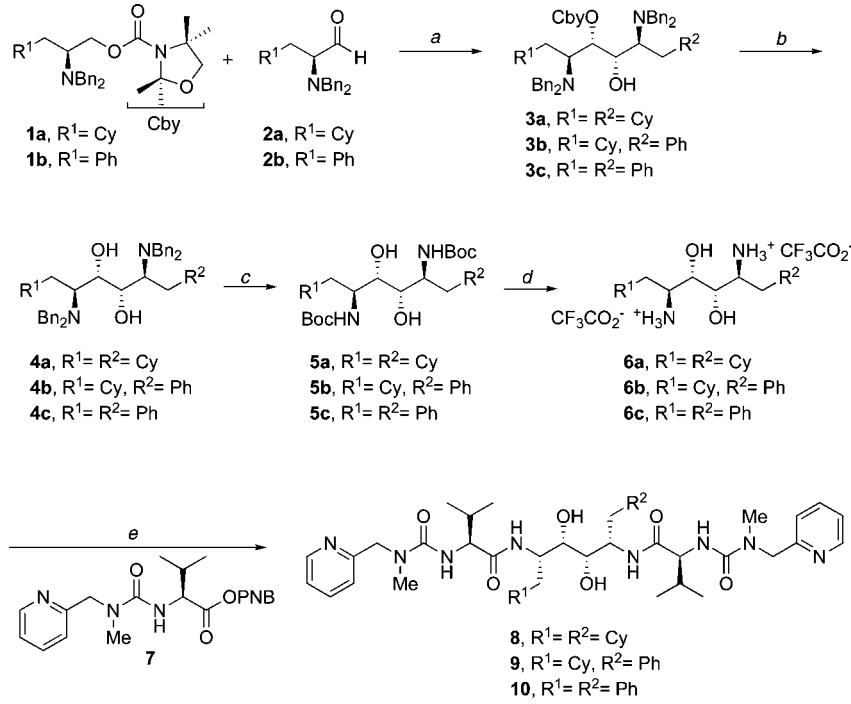

[a] Reagents and conditions: (a) 1. *s*-BuLi/TMEDA/Et_2O, −78 °C; 2. **2**/Et_2O; (b) 1. $MeSO_3H$, MeOH, reflux; 2. LiOH, dioxane/H_2O, reflux; (c) H_2, $Pd(OH)_2$/C, $(Boc)_2O$; (d) TFA; (e) K_2CO_3, THF, rt, 20 h.

HIV-1 PR mutations.[11–14] To get some insight into the binding mode of our new inhibitors to the resistant mutant V82A HIV-1 PR, we obtained the structure of the inhibitor PC bound to this variant by X-ray crystallography. The structural results provide a rationale for the better resistance profile of inhibitors **PC** and **CC**. Moreover, our crystallographic model suggests the existence of a hitherto unseen induced fit phenomenon.

Chemistry

L-Cyclohexylalanine and L-phenylalanine have been used as starting materials for the preparation of the central core of the HIV-1 protease inhibitors **CC**, **PC**, and **PP**. The synthetic approach, depicted in Scheme 1, is based on the methodology developed by Hoppe for the selective deprotonation of carbamates, followed by addition to the appropriate electrophile.[15] Thus, substrate-directed deprotonation of carbamate **1** mediated by *s*-BuLi/TMEDA,[16] followed by reaction with amino aldehyde **2**,[17] allowed the preparation of **3a** and **3b**[18] in 69% yield. Hydrolysis of the carbamate moiety to 2,5-dibenzyldiamino-3,4-diols **4** was performed by acid-catalyzed cleavage of the oxazolidine ring followed by base-catalyzed cleavage of the *N*-hydroxyalkylcarbamate intermediate (82–97% yield).[19] The *N*-benzyl protecting groups in diamines **4** were successfully removed by a two-step sequence involving $Pd(OH)_2$/C catalyzed hydrogenolysis in the presence of $(Boc)_2O$ followed by TFA treatment of the resulting dicarbamate, this sequence of reactions afforded diamino-diols **6** in 78–55% overall yield.[20] Finally, acylation of **6a**, **6b**, or **6c** with *p*-nitrophenylester **7**,[21] in the presence of K_2CO_3, gave **8**, **9**, or **10** in 36, 52, and 81% unoptimized yields, respectively.

Results and Discussion

Structural Factors behind Improved Resistance Profile. The binding constants of inhibitors **PP** (**10**), **PC** (**9**), and **CC** (**8**) with the native and V82A mutant strains of the HIV-1 PR are listed in Table 2. The results indicate that both native and mutant HIV-1 PR strains have reduced binding affinity for the Cha-containing compounds. Nevertheless, the sensitivity to the mutation, as given by the ratio of the K_i values (mutant/native) for the studied inhibitors, exhibits a pattern in which **PP** > **PC** > **CC**, indicating that the new inhibitors are less sensitive to the V82A strain. The reduced ratio in affinity between the native and mutant enzymes for the compounds containing Cha demonstrates that the Cha containing compounds are less sensitive to the V82A mutation, suggesting that this group is better able to fill the larger S1/S1′ pocket left by the V82A mutation.

Table 2. Binding Constants for the Inhibitors Bound to the Native and V82A Mutant HIV-1 PR Strains

inhibitor	K_i (nM) native	K_i (nM) mutant	K_i mutant/K_i native
PP	1.3 ± 0.2	9 ± 1	7
PC	3.2 ± 0.3	14 ± 3	4
CC	6 ± 1	12 ± 1	2

To gain an understanding about the structural modifications that make the Cha containing inhibitors less sensitive to the V82A mutation, the X-ray structure of the **PC**−HIV-1 PR^{V82A} complex was modeled and refined to 1.9 Å resolution in space group $P6_1$ (PDB entry 2FLE). When CNS-SA omit maps were used (see Experimental Section), it was not possible to assign the Phe or Cha side chain to only the S1 or S1′ pocket. This is indicative of a 2-fold (180°) bimodal binding mode that has been previously observed for other inhibitors bound to the HIV-1 PR.[1,3] To visualize the structural modifications introduced by the V82A mutation and by the replacement of a Phe side chain in P1 or P1′ by a Cha group, we have compared the structures of the **PC**−HIV-1 PR^{V82A} complex (PDB entry 2FLE) with the **PP**−HIV-1 PR^{wt} complex (PDB entry 1HVK).[10] The V82A mutation and the single side chain change in the inhibitor produced significant structural changes in the protein and the ligand, when compared to the 1HVK structure (see Figure 1). The most significant changes are located in the 80s loop of the

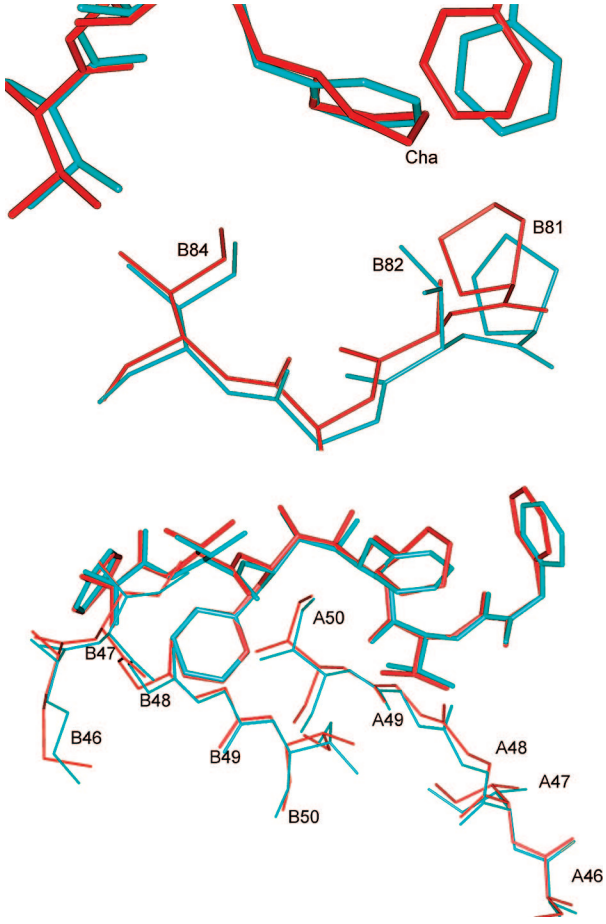

Figure 1. Some noteworthy features resulting from the superimposition of the **PP**−HIV-1 PR^{wt} (light blue) and **PC**−HIV-1 PR^{V82A} (red) complexes. The upper panel displays a close-up of the superimposed 80s loop, while the lower panel displays the superimposed flaps. The inhibitors are shown as bold sticks.

protein, a feature that was observed in other structures of inhibitors bound to the V82A HIV-1 PR variant.[22] The van der Waals contacts, below 4 Å, between the inhibitors and the active site residues for both structures are reported in Table 3. As seen from this table, some of the inhibitor−protein van der Waals contacts are lost due to V82A mutation but are compensated by the formation of a number of new ones in the **PC** bound structure, keeping the binding free energy of both complexes close. For instance, the loss of the van der Waals contacts with the Val 82 CG1 atom at residues A82 and B82 is compensated by new contacts made by the Cha fragment, like the ones with the Ala 82 CB, Pro 81 CD, Ile A50 CA, and CD1 atoms (see Table 3).

The central premise for the design of these inhibitors was that the replacement of a Phe by a bulkier Cha would help to fill the hydrophobic void left by the V82A mutation. Our results indicate that the hypothesis used for inhibitor design is satisfied experimentally. This is born out by the comparison of the shortest distances between the CB atom of Val82 to the Phe side chain and the CB atom of Ala82 to the Cha side chain. The closest atom to the CB atom (in Val82) is C44 in the Phe group at P1, located at 4.62 Å from the CB of Val B82. When the Phe group is replaced by a Cha, the closest atom to the CB (in Ala 82) is C28, from the Cha fragment at P1′, located at 3.48 Å from the CB of Ala A82, demonstrating that the Cha side chain at P1′ fills some of the empty space left by the V82A mutation.

Other protein features that differ between these two crystallographic structures are the loops involved in the flaps. As seen from the lower panel of Figure 1, the conformation of residues 46–50 change from one complex to the other, both in the main as well as in the side chains. The number of van der Waals contacts also increase in the **PC**−HIV-1 PR^{V82A} complex when compared to the **PP**−HIV-1 PR^{wt} complex (see Table 3).

Conformation of the Inhibitor Cha Group. Refinement of the model against the density data suggested that the Cha group is in a boat conformation. Restricting the Cha group to the chair conformation and refining the model against the density results in the C25 sp^3 atom adopting a highly strained angle of 121.1° compared to 113.9° for the boat conformation (Figure 2). This supports the notion that the cyclohexane exists in a boat conformation when the **PC** ligand is bound to the enzyme.

The likelihood that either the boat or the chair conformation would occur when the ligand is bound to the enzyme depends on the difference between the energy minima of these two conformations when bound to the protein in reference to the unbound conformations. In solution, the difference favors the chair over the boat conformation.[23] Binding of the inhibitor to the enzyme could shift the balance between these two conformations by stabilizing energetically either of them. For instance, a higher enzyme affinity for the boat conformation could help to compensate for the strain energy involved in docking this conformer. Because the difference in affinity for the enzyme of both the chair and the boat conformations cannot be obtained experimentally, we have estimated the values through molecular dynamics (MD)-based simulations, starting from the crystallographic structure of the inhibitor **PC** bound to the V82A HIV-1 PR variant (see Experimental Section). The calculated energy histogram suggests that the interaction energies favor the boat over the chair conformation (Figure 3). The highest ranked inhibitor's boat conformation outpaces the chair conformation by up to 10 kcal/mol. This energy difference may be sufficient to offset the internal strain energy necessary to convert the chair to the boat conformation. This ranking is borne out as well by an energy minimization protocol directly applied to the crystallographic refined structures, which indicates that the boat containing inhibitor is favored over the one with a chair by 7.0 kcal/mol (see Experimental Section).

The Cha boat conformation in the enzyme could be brought about by trying to avoid steric clashes with the pyridine fragment at P3. It has been shown previously that an increase in the size of the P3 and P3′ fragments in C_2-symmetric inhibitors with a Phe group in P1 and P1′ led to a reduction in the binding to the native HIV-1 PR, because P1 and P3 (as well as P1′ and P3′) are positioned at close quarters into pockets with limited capacity.[24] Our binding data also showed that replacement of a single Phe group at P1 or P1′ by the bulkier Cha fragment leads to a lower affinity for HIV-1 PR^{V82A} (see Table 2). We hypothesize that the reduction in affinity may be due in part to the penalty paid for the chair to boat transition in the complex affected by steric interactions with the P3 fragments. Hence, inhibitors that lack the P3 and P3′ fragments could, in principle, accommodate the Cha fragment in its chair conformation, the one preferred in solution. This could be the case of **CGP 53820**, a pseudosymmetric HIV-1 PR inhibitor with a Cha fragment in P1′, and lacking the P3′ fragment (see Table 1).[25] We have carried out MD-based calculations for this inhibitor bound to the HIV-1 PR, similar to those performed on the **PC**-bound complex described above. The starting point was the crystallographic structure of the complex (PDB entry 1HII). The results for the ligand−HIV-1 PR interaction energy distribution for the

Table 3. Van der Waals Contacts with Distances below 4 Å between the Inhibitor's Side Chain Fragments at P1/P1′ and the Protein Atoms in the Complexes **PP**−HIV-1 PR^{wt} (PDB entry 1HVK) and **PC**−HIV-1 PR^{V82A} (PDB entry 2FLE)[a]

protease atom	**PP** (Phe) atom	distance (Å)	**PC**[b] (Cha) atom	distance (Å)
Ile A84/B84 CD1	C53/C41	3.97/3.83	C31/C31	3.68/3.60
Val A82/B82 CG1	C55, C56/C43	3.95, 3.69/3.56	-	-
Val A82/B82 CG1	C57/C44	3.62/3.49	-	-
Val A82/B82 CG1	C58/C45	3.83/3.93	-	-
Ala A82/B82 CB	-	-	C28/C28	3.48/3.61
Pro A81/B81 CB	C56/-	3.85/-	C29/C29	3.83/3.82
Pro A81/B81 CG	C56/C43	3.89/3.78	-	-
Pro A81/B81 CD	-	-	C30/C30	3.82/3.85
Ile A50/B50 N	C41, C42/C55	3.78, 3.41/3.65	C30/C31	3.46/3.90
Ile A50 CA	-	-	C30	3.84
Ile A50 CD1	-	-	C30, C31	3.92, 3.90
Ile A50/B50 CG1	C41, C42/-	3.78, 3.81/-	-/C31	-/3.83
Gly B49 N	-	-	C30	3.51
Gly A49/B49 CA	C42/C55	3.91/3.93	C30/C30	3.94/3.63
Gly A49/B49 C	C42/C55	3.71/3.71	C30/C30	3.50/3.58
Gly A49 O	-	-	C30	3.87
Leu A23/B23 CD2	-	-	C27/C27	3.82/3.93

[a] The slash (/) is used to differentiate the contacts between the chains A and B of the protein. In those cases where, in the same row, there are more than one atom contacts for the inhibitor, we use commas (,) for the separation. [b] In this case, the van der Waals distances are for the same Cha fragment in the two orientations of the inhibitor inside the protein.

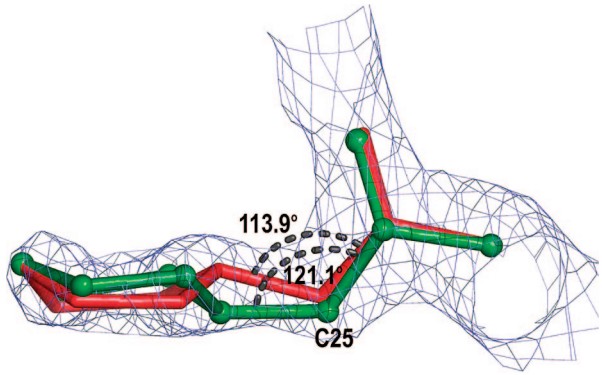

Figure 2. Overlap of the Cha side chain boat (in red) and chair (in green) models resulting from the refinement protocol of the crystal structure of the **PC** ligand bound to the V82A mutant of HIV-1 PR. $2F_o - F_c$ density at 1.5 σ is drawn as a blue mesh. Valence angles for C25 in both conformations are shown in black.

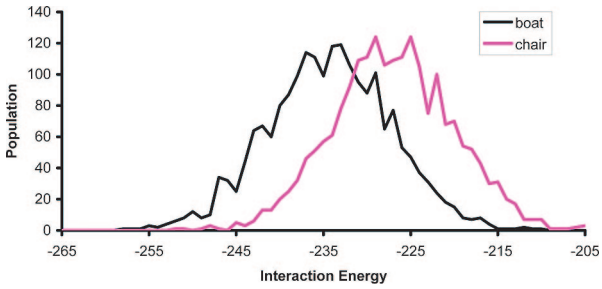

Figure 3. Ligand−HIV-1 protease interaction energy histogram obtained from the production stage of the MD simulations of the complex between the V82A protease variant and the **PC** inhibitor with the Cha fragment in its boat conformation (black) and the chair conformation (indigo).

Cha in its boat and chair conformation are shown in Figure 4. These results indicate that the interaction energy favors the chair over the boat conformation. Comparison of the ligand−protein interaction energy histograms shown in Figures 3 and 4 suggests that the presence of P3/P3′ fragments may be essential for selecting the boat conformation for the P1/P1′ fragment of **PC** when bound to the HIV-1 PR. In principle, the larger pocket created by the V82A mutation could influence the chair/boat equilibrium by accommodating better the chair conformation, but our results indicate that this is not the case.

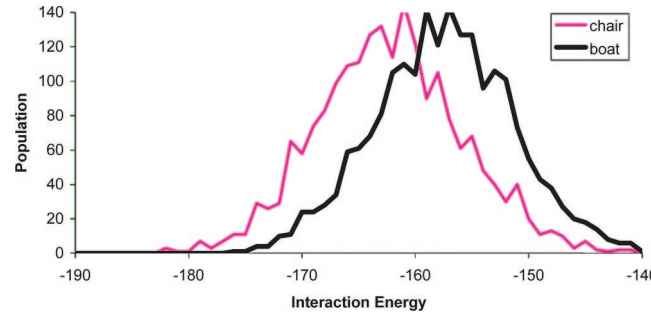

Figure 4. Ligand−HIV-1 protease interaction energy histogram obtained from the production stage of MD simulations of the complex between the native HIV-1 PR and the **CGP 53820** inhibitor with the Cha fragment in its boat conformation (black) and chair conformation (indigo).

In general, ligands rarely bind in their lowest energy conformation, and in many cases the bound conformation of the ligand is at least 5 kcal/mol above its absolute minimum in the unbound conformation in solution.[26] Nevertheless, to the best of our knowledge, this is the first report of a possible enzyme "trapping" a cyclohexane in a boat conformation through an induced-fit process.[27,28]

Conclusions

We have designed, synthesized, and tested a set of almost C_2-symmetric HIV-1 PR inhibitors, with a Cha group in P1, P1′, or both. The design objective was to compensate for the hydrophobic cavity created in the S1/S1′ pocket by the V82A mutation. The binding data indicates that the second generation inhibitors are less sensitive to the V82A mutation, in agreement with our working hypothesis. To understand the structural features underlying the response of these inhibitors for the V82A mutation, we have solved the structure of the **PC** inhibitor bound to the V82A HIV-1 PR by X-ray crystallography. Comparison of this structure with that of the **PP** inhibitor bound to the native HIV-1 PR indicates that the Cha group fills at least in part the void left by the V82A mutation. An analysis of the alternative ring conformations in the Cha group indicates the possibility that this group may adopt the boat rather than the chair conformation, which is prevalent in solution. MD simulations support the conformation assignment and provide a rationale for this outcome, indicating that the boat conformation can result

from avoidance of steric clashes of the Cha group with the pyridine fragment at P3/P3′. The existence of an induced-fit phenomenon of this kind would have to be validated through high resolution X-ray structures or neutron diffraction studies.

Experimental Section

Chemistry. General. All reactions were performed under an inert atmosphere of dry argon in glassware that had been oven-dried or flame-dried. Reaction temperatures are reported as the temperature of the bath surrounding the vessel. Tetrahydrofuran (THF) and diethyl ether (Et_2O) were distilled from sodium/benzophenone immediately before use, methylene chloride (CH_2Cl_2), EtOAc, triethylamine, tetramethylethylenediamine (TMEDA), and DMSO were distilled from CaH_2, and methanol was distilled from $Mg(OMe)_2$. NMR spectra were recorded in $CDCl_3$ unless otherwise noted. Chemical shifts are reported in ppm (δ) relative to the internal TMS (tetramethylsilane) reference signal. J values are reported in hertz (Hz). Final solutions were dried over anhydrous Na_2SO_4 before evaporation. 2,2,4,4-Tetramethyl-1,3-oxazolidine,[29] 2,2,4,4-tetramethyl-1,3-oxazolidine-3-carbonyl chloride[29] (CbyCl), **1b**,[30] **2a**,[17b] **2b**,[17a] **3c**,[18] **4c**,[18] and **7**[21] were prepared according to the literature.

(2*S*)-3-Cyclohexyl-2-(dibenzylamino)propyl 2,2,4,4-tetramethyl-1,3-oxazolidine-3-carboxylate (1a). To a suspension of NaH (265 mg, 6.65 mmol) in THF (5 mL), a solution of (2*S*)-3-cyclohexyl-2-(dibenzylamino)propan-1-ol[17b] (1.50 g, 4.44 mmol) in THF (2.5 mL) was added, and the resulting mixture was stirred at rt for 30 min. A solution of CbyCl (1.02 g, 5.33 mmol) in THF (2 mL) was added and then stirred at rt for 5 days. The reaction was quenched by addition of 2 M HCl to reach pH 7 and then extracted with EtOAc (3 × 15 mL). The combined organic phase was washed with satd aq $NaHCO_3$ (30 mL), H_2O (30 mL), and brine (30 mL), dried, and evaporated to give **1a**, after column chromatography (SiO_2, EtOAc/hexane 1:15), as a colorless oil (1.73 g, 79% yield, 97% based on recovered starting material): $[\alpha]^{22}_D$ −22.6° (*c* 1.25, CH_2Cl_2); IR (NaCl) 1695 cm^{-1}; ^1H NMR (rotamers) δ 7.32 (m, 10H), 4.36 (m, 1H), 4.13 (m, 1H), 3.79 (m, 4H), 3.60 (d, J = 13.9, 2H), 2.99 (m, 1H), 1.75–1.05 (m, 23H), 0.92 (m, 1H), 0.62 (m, 1H); ^{13}C NMR (rotamers) δ 152.7 and 152.0, 140.0, 128.8, 127.9, 126.7, 95.8 and 94.5, 76.2 and 75.8, 60.6 and 59.4, 53.6 and 53.0, 36.84 and 36.78, 34.0, 33.8, 32.6, 26.44, 26.40, 26.0, 25.34, 25.28, 25.12, 25.07, 24.0. Anal. ($C_{31}H_{44}N_2O_3$) C, H, N.

(2*S*,3*S*,4*S*,5*S*)-1,6-Dicyclohexyl-2,5-bis(dibenzylamino)-4-hydroxyhexan-3-yl 2,2,4,4-tetramethyl-1,3-oxazolidine-3-carboxylate (3a). To a solution of **1a** (435 mg, 0.88 mmol) and TMEDA (200 μL, 1.32 mmol) in Et_2O (7 mL) at −78 °C was added *s*-BuLi (1.0 mL, 1.32 mmol, 1.3 M in cyclohexane). The resulting solution was stirred at −78 °C for 5 h, and then treated with a solution of aldehyde **2a** (444 mg, 1.32 mmol) in Et_2O (6 mL). The resulting mixture was stirred for 1.5 h at −78 °C, then the cooling bath was removed and stirring was continued for an additional 30 min. The mixture was partitioned between H_2O (20 mL) and EtOAc (30 mL). The organic layer was washed with brine, dried, filtered, and evaporated to give a residue that was purified by column chromatography (SiO_2, EtOAc/hexane 1:8) to yield **3a** as a white foam (505 mg, 69%): $[\alpha]^{20}_D$ −42.4° (*c* 1.0, CH_2Cl_2); IR (CsI) 1692 cm^{-1}; ^1H NMR (rotamers) δ 7.21 (m, 20H), 5.37 (bs, 1H), 4.16 (bs, 1H), 3.92–3.20 (m, 11 H), 2.85 (m, 1H), 2.66 (bd, J = 9.7, 1H), 1.77–0.76 (m, 36H), 0.04 (m, 2H); ^{13}C NMR (rotamers) δ 152.9, 152.2, 140.6, 140.2, 139.3, 128.9, 128.4, 128.3, 128.2, 128.0, 127.0, 126.8, 126.6, 96.1, 94.7, 76.2, 75.8, 75.4, 71.6, 61.0, 59.7, 55.9, 55.6, 55.5, 54.4, 54.2, 54.1, 53.6, 52.9, 35.1, 35.0, 34.7, 34.5, 34.4, 34.2, 33.4, 33.2, 32.8, 32.4, 31.5, 31.2, 27.2, 26.8, 26.7, 26.4, 26.3, 26.0, 25.9, 25.4, 24.8, 24.3, 24.1. Anal. ($C_{54}H_{73}N_3O_4$) C, H, N.

(2*S*,3*S*,4*S*,5*S*)-6-Cyclohexyl-2,5-bis(dibenzylamino)-4-hydroxy-1-phenylhexan-3-yl 2,2,4,4-tetramethyl-1,3-oxazolidine-3-carboxylate (3b) and (2*S*,3*S*,4*S*,5*S*)-1-Cyclohexyl-2,5-bis(dibenzylamino)-4-hydroxy-6-phenylhexan-3-yl 2,2,4,4-tetramethyl-1,3-oxazolidine-3-carboxylate (3b′). A solution of **1b** (739 mg, 1.52 mmol) and TMEDA (342 μL, 2.28 mmol) in Et_2O (11 mL) at −78 °C was treated with *s*-BuLi (1.90 mL, 2.28 mmol, 1.2 M in cyclohexane). The resulting solution was stirred at −78 °C for 5 h, then treated with a solution of aminoaldehyde **2a** (764 mg, 2.28 mmol) in Et_2O (11 mL) and stirred for 1.5 h. The cooling bath was removed and stirred for 30 min, then partitioned between EtOAc (20 mL) and H_2O (30 mL). The organic phase was washed with brine (3 × 20 mL), dried, and evaporated to give a mixture of two isomers, arising from a partial migration of the Cby group to the newly introduced hydroxyl group in the basic reaction medium, in a 60/40 ratio. Column chromatography (SiO_2, EtOAc/hexane 1:8) gave **3** in a combined yield of 69% (861 mg). Main isomer: 499 mg of **3b** as a white foam (40%): $[\alpha]^{23}_D$ −27.9° (*c* 1.1, CH_2Cl_2); IR (NaCl) 1732 cm^{-1}; ^1H NMR (C_6D_6, rotamers) δ 7.38 (d, J = 7.0, 4H), 7.23–6.98 (m, 21H), 5.70 (bs, 1H), 4.45 (bs, 1H), 4.01 (d, J = 14.0, 2H), 3.81 (d, J = 7.0, 4H), 3.66 (d, J = 14.0, 2H), 3.44 (m, 3H), 3.15 (m, 1H), 3.00 (m, 2H), 1.80–0.81 (m, 25H), 0.28 (m, 1H); ^{13}C NMR (rotamers) δ 152.9, 152.2, 140.4, 139.7, 139.6, 129.8, 128.7, 128.3, 128.2, 128.1, 128.0, 126.8, 126.7, 126.2, 96.3, 94.9, 76.3, 76.0, 75.5, 75.4, 71.0, 70.9, 61.2, 60.0, 59.0, 58.9, 55.9, 55.8, 54.6, 53.7, 34.4, 33.7, 33.4, 33.3, 31.2, 27.3, 27.0, 26.9, 26.3, 26.1, 25.8, 25.7, 25.1, 24.4, 24.2. Anal. ($C_{54}H_{67}N_3O_4$) C, H, N. Minor isomer: 362 mg of **3b′** as a white foam (29%): $[\alpha]^{20}_D$ −17.3° (*c* 1.5, CH_2Cl_2); IR (NaCl) 1689 cm^{-1}; ^1H NMR (C_6D_6, rotamers) δ 7.39 (m, 5H), 7.20–6.98 (m, 20H), 5.75 (bs, 1H), 4.37 (bs, 1H), 3.91 (m, 4H), 3.77 (m, 4H), 3.37 (m, 3H), 3.20 (m, 2H), 3.00 (t, J = 12.2, 1H), 2.80 (dd, J = 3.1 and 13.9, 1H), 1.89–0.81 (m, 24 H), 0.27 (m, 1H); ^{13}C NMR (rotamers) δ 153.1, 152.4, 140.03, 140.01, 129.9, 128.7, 128.3, 128.0, 127.9, 126.9, 126.5, 125.8, 96.3, 94.9, 76.3, 76.0, 72.3, 72.2, 61.18, 61.15, 61.0, 59.9, 54.5, 54.3, 54.2, 53.8, 35.4, 35.3, 34.6, 33.59, 33.56, 32.3, 32.2, 31.6, 31.5, 27.2, 26.9, 26.8, 26.34, 26.32, 26.1, 26.0, 25.4, 24.9, 24.4, 24.3. Anal. ($C_{54}H_{67}N_3O_4$) C, H, N.

(2*S*,3*S*,4*S*,5*S*)-1,6-Dicyclohexyl-2,5-bis(dibenzylamino)hexane-3,4-diol (4a). A solution of **3a** (485 mg, 0.59 mmol) and $MeSO_3H$ (305 μL, 2.93 mmol) in MeOH (7 mL) was refluxed for 16 h in a sealed tube. After cooling to rt, it was treated with a mixture of $LiOH \cdot H_2O$ (197 mg, 4.68 mmol), dioxane (7 mL), and H_2O (7 mL). The resulting mixture was refluxed for 2 h, cooled to rt, diluted with CH_2Cl_2 (15 mL), and neutralized with 10% H_3PO_4. The organic layer was washed with H_2O (15 mL) and brine (15 mL), dried, filtered, and evaporated to give a residue which was chromatographed (SiO_2, EtOAc/hexane 1:6) to yield **4a** as a white foam (323 mg, 82%): $[\alpha]^{20}_D$ −18.4° (*c* 1.0, CH_2Cl_2); ^1H NMR δ 7.27 (m, 20H), 3.90 (d, J = 4.3, 2H), 3.71 (d, J = 14.3, 4H), 3.64 (d, J = 14.3, 4H), 2.78 (m, 2H), 2.27 (bs, 2H), 1.75–1.12 (m, 22H), 0.93 (m, 2H), 0.75 (m, 2H); ^{13}C NMR δ 140.1, 128.8, 128.2, 126.9, 71.4, 56.7, 54.5, 34.6, 34.4, 33.9, 33.5, 26.6, 26.5, 26.2. Anal. ($C_{46}H_{60}N_2O_2$) C, H, N.

(2*S*,3*S*,4*S*,5*S*)-6-Cyclohexyl-2,5-bis(dibenzylamino)-1-phenylhexane-3,4-diol (4b). Same procedure as above applied to both isomers **3b** and **3b′** yielded the same product **4b** in 97% yield: $[\alpha]^{22}_D$ −6.8° (*c* 1.2, CH_2Cl_2); ^1H NMR δ 7.23–7.07 (m,

25H), 3.90 (d, $J = 3.8$, 1H), 3.86 (d, $J = 6.3$, 1H), 3.65 (d, $J = 13.3$, 2H), 3.54 (t, $J = 14.3$, 4H), 3.49 (d, $J = 13.3$, 2H), 2.98 (m, 3H), 2.69 (q, $J = 6.4$, 1H), 1.97 (bs, 2H), 1.64–1.39 (m, 7H), 1.27 (m, 1H), 1.19–1.04 (m, 3H), 0.81 (m, 1H), 0.66 (m, 1H); ^{13}C NMR δ 141.6, 140.0, 139.6, 129.7, 128.9, 128.7, 128.3, 128.2, 127.03, 127.01, 125.8, 72.2, 71.9, 61.9, 56.5, 54.7, 54.6, 34.9, 34.0, 33.6, 32.8, 26.7, 26.5, 26.3. Anal. ($C_{46}H_{54}N_2O_2$) C, H, N.

(2*S*,3*S*,4*S*,5*S*)-2,5-Bis[(*tert*-butoxycarbonyl)amino]-1,6-dicyclohexylhexane-3,4-diol (5a). To a deoxygenated solution of **4a** (292 mg, 0.43 mmol) and $(Boc)_2O$ (260 mg, 1.19 mmol) in EtOAc (10 mL) was added 20% $Pd(OH)_2/C$ (117 mg), and the mixture was stirred under hydrogen for 4 days. The catalyst was removed by filtration through Celite and washed thoroughly with EtOAc and warm CH_2Cl_2. The filtrate and washings were evaporated to give a white solid that was recrystallized from CH_2Cl_2/EtOH (137 mg). The mother liquors were evaporated and the residue was chromatographed (SiO_2, EtOAc/hexane 1:6 to 1:3) to yield 36 mg of **5a** (173 mg, 78% combined yield): mp 239–241 °C (CH_2Cl_2/EtOH); $[\alpha]^{20}_D$ −50.8° (*c* 0.5, CH_2Cl_2); IR (CsI) 1662 cm^{-1}; ^{1}H NMR δ 4.47 (d, $J = 8.8$, 2H), 3.74 (m, 4H), 3.27 (m, 2H), 1.88–1.54 (m, 10H), 1.44 (s, 18H), 1.50–0.75 (m, 16H); ^{13}C NMR δ 157.2, 80.0, 73.0, 50.0, 39.5, 34.3, 32.2, 28.3, 26.5, 26.4, 26.1. Anal. ($C_{28}H_{52}N_2O_6$) C, H, N.

(2*S*,3*S*,4*S*,5*S*)-2,5-Bis[(*tert*-butoxycarbonyl)amino]-6-cyclohexyl-1-phenylhexane-3,4-diol (5b). Following the above procedure, 209 mg of **5b** (55% yield) was prepared from **4b** (500 mg, 0.75 mmol) as a white solid after recrystallization from CH_2Cl_2/EtOH: mp 210–212 °C (CH_2Cl_2/EtOH); $[\alpha]^{25}_D$ −26.4° (*c* 1.0, CH_2Cl_2); IR (CsI) 1664 cm^{-1}; ^{1}H NMR δ 7.25 (m, 5H), 4.53 (d, $J = 8.8$, 1H), 4.30 (d, $J = 6.1$, 2H), 4.01 (m, 1H), 3.85 (d, $J = 4.8$, 1H), 3.71 (m, 1H), 3.32 (m, 1H), 3.13 (m, 2H), 2.98 (dd, $J = 3.6$ and 13.4, 1H), 1.99–0.76 (m, 13H), 1.45 (s, 9H), 1.38 (s, 9H); ^{13}C NMR δ 157.3, 156.8, 137.4, 129.8, 128.5, 126.4, 80.2, 80.1, 73.1, 70.3, 51.4, 49.6, 39.7, 36.4, 34.3, 32.1, 28.34, 28.27, 26.5, 26.4, 26.1. Anal. ($C_{28}H_{46}N_2O_6$) C, H, N.

(2*S*,3*S*,4*S*,5*S*)-2,5-Bis[(*tert*-butoxycarbonyl)amino]-1,6-diphenylhexane-3,4-diol (5c).[20] Following the same procedure as for **5a**, **5c** was prepared from **4c** (1.37 g, 2.07 mmol) in 74% yield (767 mg) as a white solid after recrystallization: mp 213–215 °C (CH_2Cl_2/EtOH); $[\alpha]^{25}_D$ −13.4° (*c* 1.0, CH_2Cl_2); IR (CsI) 1662 cm^{-1}; ^{1}H NMR δ 7.22 (m, 10H), 4.42 (m, 4H), 4.02 (m, 2H), 3.20 (m, 4H), 2.97 (dd, $J = 4.3$ and 13.7, 2H), 1.41 (s, 18H); ^{13}C NMR δ 156.9, 137.0, 129.8, 128.6, 126.5, 80.2, 70.1, 50.8, 36.3, 28.3. Anal. ($C_{28}H_{40}N_2O_6$) C, H, N.

(2*S*,3*S*,4*S*,5*S*)-2,5-Diamino-1,6-dicyclohexylhexane-3,4-diol Bistrifluoracetate (6a). A solution of **5a** (150 mg, 0.29 mmol) in TFA−CH_2Cl_2 (1:2, 6 mL) was stirred for 15 min at rt and then evaporated to give a pale yellow foam (158 mg, 100%) that was used without further purification: ^{1}H NMR (CD_3OD) δ 4.02 (d, $J = 3.9$, 2H), 3.44 (m, 2H), 1.86–0.69 (m, 22H), 0.97 (m, 4H); ^{13}C NMR (CD_3OD) δ 161.5 (q, $J_{C-F} = 37.3$), 117.3 (q, $J_{C-F} = 289.4$), 69.0, 54.5, 37.6, 35.0, 34.2, 33.9, 27.4, 27.2, 27.1.

(2*S*,3*S*,4*S*,5*S*)-2,5-Diamino-6-cyclohexyl-1-phenylhexane-3,4-diol Bistrifluoroacetate (6b). Following the same procedure as above, **6b** was prepared from **5b** (100 mg, 0.20 mmol) as a pale yellow foam in quantitative yield (105 mg): ^{1}H NMR (CD_3OD) δ 7.35 (m, 5H), 4.15 (m, 1H), 3.87 (m, 1H), 3.78 (m, 1H), 3.42 (m, 1H), 3.21 (dd, $J = 6.6$, 14.2, 1H), 2.99 (dd, $J = 9.6$, 14.2, 1H), 1.81–1.06 (m, 10H), 0.88 (m, 3H); ^{13}C NMR (CD_3OD) δ 158.8 (q, $J_{C-F} = 41.7$), 136.4, 130.1, 129.7, 128.3, 115.8 (q, $J_{C-F} = 283.9$), 68.2, 67.8, 57.8, 54.5, 37.6, 35.9, 34.32, 34.27, 33.6, 27.3, 26.8, 26.7.

(2*S*,3*S*,4*S*,5*S*)-2,5-Diamino-1,6-diphenylhexane-3,4-diol Bistrifluoracetate (6c). Following the same procedure as above, **6c** was prepared from 286 mg of **5c** (0.57 mmol) in quantitative yield (302 mg): ^{1}H NMR (CD_3OD) δ 7.29 (m, 6H), 7.17 (m, 4H), 4.09 (d, $J = 3.1$, 2H), 3.70 (m, 2H), 3.02 (dd, $J = 7.1$, 14.3, 2H), 2.89 (dd, $J = 8.4$, 14.3, 2H); ^{13}C NMR (CD_3OD) δ 162.7 (q, $J_{C-F} = 35.5$), 136.5, 130.2, 129.7, 128.5, 118.0 (q, $J_{C-F} = 290.7$), 68.4, 58.4, 35.8.

(2*S*,3*S*,4*S*,5*S*)-2,5-Bis[*N*-[*N*-[[*N*-methyl-*N*-(2-pyridinylmethyl)amino]carbonyl]valinyl] amino]-1,6-dicyclohexylhexane-3,4-diol (8). A solution of **7**[21] (132 mg, 0.34 mmol) in THF (1.6 mL) was added to a mixture of **6a** (74 mg, 0.14 mmol) and K_2CO_3 (38 mg, 0.27 mmol) in THF (1.6 mL). The resulting mixture was stirred at room temperature for 20 h, diluted with H_2O (1 mL), basified to pH 12 with 1 M NaOH, and stirred for an additional hour. The mixture was partitioned between H_2O (5 mL) and EtOAc (2 × 10 mL). The combined organic phase was washed with satd aq K_2CO_3 (5 × 5 mL), dried, evaporated, and purified by column chromatography (SiO_2, CH_2Cl_2/Et_2O 90:10 to $CHCl_3$/MeOH 95:5) to yield **8** as a white solid, which was recrystallized from CH_2Cl_2/Et_2O (40 mg, 36%): mp 136–138 °C (CH_2Cl_2/Et_2O); $[\alpha]^{25}_D$ −11.2° (*c* 1.0, CH_2Cl_2); IR (CsI) 1655, 1633, 1522 cm^{-1}; ^{1}H NMR δ 8.55 (d, $J = 4.7$, 2H), 7.74 (bt, $J = 7.1$, 2H), 7.31 (bd, $J = 7.9$, 2H), 7.27 (m, 2H), 6.73 (bs, 2H), 6.39 (bs, 2H), 4.66 (bd, $J = 12.4$, 2H), 4.43 (d, $J = 15.9$, 2H), 4.08 (m, 2H), 4.04 (bt, $J = 6.4$, 2H), 3.42 (d, $J = 6.0$, 2H), 3.01 (s, 6H), 2.32 (oct, $J = 6.7$, 2H), 1.76 (bd, $J = 12.7$, 2H), 1.63 (m, 10H), 1.29 (m, 4H), 1.21–0.81 (m, 10H), 0.99 (d, $J = 7.0$, 6H), 0.97 (d, $J = 7.0$, 6H); ^{13}C NMR δ 173.8, 159.2, 157.2, 149.3, 137.4, 122.9, 122.5, 72.0, 60.3, 54.9 (CH_2), 49.1, 39.3 (CH_2), 35.2, 34.3, 34.0 (CH_2), 32.0 (CH_2), 29.4, 26.42 (CH_2), 26.39 (CH_2), 26.1 (CH_2), 19.7, 17.4. Anal. ($C_{44}H_{70}N_8O_6 \cdot H_2O$) C, H, N.

(2*S*,3*S*,4*S*,5*S*)-2,5-Bis[*N*-[*N*-[[*N*-methyl-*N*-(2-pyridinylmethyl)amino]carbonyl]valinyl] amino]-6-cyclohexyl-1-phenylhexane-3,4-diol (9). A total of 88 mg of **9** (52% yield) was obtained as a white solid from **7**[21] (191 mg, 0.49 mmol) and **6b** (105 mg, 0.20 mmol) by following the same procedure as for **8**: mp 106–108 °C (CH_2Cl_2/Et_2O); $[\alpha]^{25}_D$ +10.6° (*c* 1.0, CH_2Cl_2); IR (CsI) 1647, 1572 cm^{-1}; ^{1}H NMR δ 8.58 (m, 2H), 7.85 (m, 2H), 7.38 (m, 4H), 7.21 (m, 4H), 7.12 (m, 1H), 6.36 (bs, 1H), 6.18 (bs, 1H), 4.88 (bs, 2H), 4.36 (m, 3H), 4.14 (m, 1H), 3.96 (bs, 2H), 3.56 (bs, 2H), 3.02 (s, 3H), 3.00 (s, 3H), 2.98 (m, 1H), 2.90 (dd, $J = 8.4$ and 14.1, 1H), 2.30 (oct, $J = 6.7$, 1H), 2.22 (oct, $J = 6.7$, 1H), 1.77 (d, $J = 13.0$, 2H), 1.68–1.42 (m, 6H), 1.25 (m, 2H), 1.12 (m, 3H), 0.98 (m, 6H), 0.85 (d, $J = 6.8$, 3H), 0.79 (d, $J = 6.8$, 3H); ^{13}C NMR δ 174.0, 173.9, 159.2, 159.0, 157.2, 157.0, 149.3, 149.2, 138.3, 137.4, 137.3, 129.1, 128.4, 126.2, 123.0, 122.9, 122.7, 122.4, 72.1, 70.7, 60.3, 59.8, 54.9 (CH_2), 54.8 (CH_2), 52.7, 49.0, 39.4 (CH_2), 37.6 (CH_2), 35.2, 35.1, 34.3, 34.1 (CH_2), 31.8 (CH_2), 29.5, 29.3, 26.4 (CH_2), 26.3 (CH_2), 25.9 (CH_2), 19.8, 19.4, 17.4, 16.5. Anal. ($C_{44}H_{64}N_8O_6 \cdot 1.5H_2O$) C, H, N.

(2*S*,3*S*,4*S*,5*S*)-2,5-Bis[*N*-[*N*-[[*N*-methyl-*N*-(2-pyridinylmethyl)amino]carbonyl]valinyl] amino]-1,6-diphenylhexane-3,4-diol (10). A mixture of **6c** (200 mg, 0.40 mmol) and K_2CO_3 (110 mg, 0.80 mmol) in THF (1.5 mL) at 0 °C was treated with a solution of **7**[21] (217 mg, 0.66 mmol) in THF (2 mL). The resulting mixture was stirred at 0 °C for 10 h, then warmed to rt, and stirred for an additional 10 h. A second addition of **7** (200 mg, 0.61 mmol) in THF (2 mL) was carried out, and the resulting mixture was stirred for 20 h at room temperature. H_2O (2 mL) was added, followed by 1 M NaOH until pH 12 was reached, and then stirred for an additional hour. The reaction

mixture was extracted with EtOAc (2 × 15 mL), the combined organic phase was washed with satd aq K_2CO_3 (5 × 10 mL), dried, evaporated, and chromatographed (SiO_2, CH_2Cl_2/Et_2O 90:10 to $CHCl_3$/MeOH 95:5) to give **10** as a white solid (256 mg, 81%), which was recrystallized from CH_2Cl_2/Et_2O: mp 110 °C (softens) (CH_2Cl_2/Et_2O); $[\alpha]^{25}_D$ +28.0° (*c* 1.0, CH_2Cl_2); IR (CsI) 1646, 1571 cm^{-1}; ^1H NMR δ 8.53 (d, J = 4.6, 2H), 7.74 (t, J = 7.1, 2H), 7.27 (m, 4H), 7.16 (m, 8H), 7.09 (m, 2H), 6.73 (bs, 2H), 6.14 (bs, 2H), 4.59 (bd, J = 15.9, 2H), 4.35 (d, J = 15.9, 2H), 4.31 (m, 2H), 4.08 (dd, J = 5.4 and 7.1, 2H), 3.46 (d, J = 8.0, 2H), 3.20 (dd, J = 4.2 and 14.2, 2H), 2.96 (s, 6H), 2.77 (dd, J = 9.0 and 14.3, 2H), 2.23 (oct, J = 6.8, 2H), 0.85 (d, J = 6.7, 6H), 0.72 (d, J = 6.7, 6H); ^{13}C NMR δ 174.0, 159.1, 157.0, 149.3, 138.7, 137.4, 129.2, 128.3, 126.1, 123.0, 122.4, 71.4, 59.9, 54.7 (CH_2), 52.1, 37.5 (CH_2), 35.1, 29.3, 19.4, 16.3. Anal. ($C_{44}H_{58}N_8O_6 \cdot H_2O$) C, H, N.

Mutagenesis and Expression of the Protease. A complete description of the cloning, expression, and purification procedures can be found in Ido et al.[31] and Goodenow et al.[32] In brief, the HIV-1 protease DNA was subcloned into the pET23a expression vector (Novagen).[33] The construct was transformed into the *E. coli* strain BL21 Star DE3 PlysS from Invitrogen. The V82A mutation was introduced into the HIV-PR background using the QuikChange Mutagenesis Kit from Stratagene. Protease expression in bacteria was initiated when the OD_{600} reached 0.6 by addition of 1 mM IPTG to a culture grown at 37 °C in M9 Media (6.8 g Na_2HPO_4, 3 g KH_2PO_4, 0.5 g NaCl, 1 g NH_4SO_4, and 5 g casamino acids were autoclaved together in 987 mL of H_2O, and then 1 mL of 0.1 M $CaCl_2$, 2 mL of 1.0 M $MgSO_4$, 10 mL of 20% glucose, and 50 μg/L of ampicillin were added). After three hours, cells were harvested by centrifugation at 16000 *g* for five minutes and resuspended in TN buffer (0.05 M Tris, 0.15 M NaCl, 0.001 M $MgCl_2$, pH 7.4). Inclusion bodies containing the protease were isolated by centrifugation through a 27% sucrose cushion. The inclusion bodies were solubilized in 8 M urea, and the protease was refolded by dialysis against 0.05 M sodium phosphate buffer (0.05 M Na_2HPO_4, 0.005 M EDTA, 0.3 M NaCl, and 0.001 M dTT, pH 7.3). The protease was purified through ammonium sulfate precipitation and gel filtration chromatography using a Superdex 75 16/60 column from Amersham Pharmacia attached to an FPLC LCC 500 Plus, also from Pharmacia. The protease was eluted using potassium phosphate buffer (50 mM K_2HPO_4, 2 mM EDTA, 150 mM NaCl, 2 mM dTT, 5% glycerol, and 5% isopropanol, pH 7.3).

Determination of Inhibition Constants. K_i values were determined for each inhibitor with the HIV-PR strains as previously described.[34] Cleavage of the chromogenic substrate (K-A-R-V-*L**Nph-E-A-nL-G, Nph = *p*-nitrophenylalanine, nL = norleucine) was monitored using a Hewlett-Packard 8452A spectrophotometer equipped with a seven-cell sample handling system at 37 °C in sodium acetate buffer (0.05 M NaOAc, 0.15 M NaCl, 0.002 M EDTA, 0.001 M dTT, pH 4.7), as described by Dunn et al.[35] The inhibition constants K_i were determined by monitoring the inhibition of hydrolysis of the chromogenic substrate, as described by Bhatt et al.[36]

Crystallization of Protein−Inhibitor Complex. After the HIV-PR^{V82A} was purified, the enzyme purification buffer was exchanged for 50 mM sodium acetate, 1 mM EDTA, and 1 mM dTT at pH 4.7 during concentration to 2 mg/mL. The inhibitor **PC** was dissolved at a concentration of 20 mM in 100% DMSO and mixed with the HIV- PR^{V82A} in a molar ratio of 3:1. The inhibitor and enzyme were allowed to equilibrate for one hour at 4 °C, after which precipitated material was removed by centrifugation at 10000 *g* at 4 °C. The enzyme–inhibitor complex was mixed with reservoir solution (Hampton Research Cryo Crystallization Kit #18) in a 1:1 (v/v) ratio to set up 4 μL hanging drops at 25 °C. Rod-shaped crystals grew in two days.

Table 4. Crystallographic Statistics

Data Collection Statistics	
wavelength (Å)	1.1
resolution range (Å)	20–1.9
space group	$P6_1$
unit-cell parameters *a*, *c* (Å)	62.2, 82.8
number of reflections	76487
number of unique reflections	14390
overall completeness (%)	100 (100)
average *I*/s	13.3
R_{sym} (%)[a]	7.1 (48.6)
Refinement Statistics	
R_{work} (%)[b]	19.9 (22.5)
R_{free} (%)[c]	23.5 (26.8)
rmsd bond length (Å)	0.009
rmsd bond angle (deg)	1.5
Average *B* Factor (Å^2)	
protein main/side chains	30.7/35.7
inhibitor atoms	32.1
water molecules	39.5
Ramachandran Plot Quality	
most favored (%)	94.9
additionally allowed (%)	5.1
generally allowed (%)	0
disallowed (%)	0

[a] $R_{sym} = \sum_{hkl}(|\langle I(hkl)\rangle - I_i(hkl)|/\langle I_i(hkl)\rangle)\times 100$, where $I_i(hkl)$ is the *i*th observation of the intensity of a reflection with indices *h*, *k*, and *l* and $\langle I(hkl)\rangle$ is the average intensity of all symmetry equivalent measurements of those reflections. [b] $R_{work} = \sum_{hkl}(F_{obs}(hkl) - F_{calc}(hkl))/F_{obs}(hkl)\times 100$, where $F_{obs}(hkl)$ and $F_{calc}(hkl)$ are the observed and calculated structure factor amplitudes respectively. [c] R_{free} was calculated using 5% of data excluded during the refinement process. In parenthesis is the highest resolution shell.

X-ray Data Collection, Structure Determination, and Refinement. X-ray diffraction images were collected at 100 K at the Brookhaven National Laboratory beamline X29 on an ADSC quantum 315 CCD detector. The crystal was dipped in cryoprotectant solution (30% glycerol in reservoir solution) prior to data collection. A complete data set was collected from a single crystal. The data were indexed, scaled, and reduced using DENZO and SCALEPACK.[37] The complex crystallized in the $P6_1$ space group.

Molecular replacement was used to calculate initial phases employing the coordinates of PDB entry 1SGU as a search model after removing inhibitor and waters. Standard methods of structure refinement were then employed using programs in the CNS Suite.[38] Electron density maps with coefficients $2F_o-F_c$ and F_o-F_c were used to guide manual fitting of the protease and bound inhibitor followed by real space refinement using the molecular graphics program WinCoot.[39] The inhibitor and water molecules were initially modeled into F_o-F_c density at 2σ. Detailed refinements of the cyclohexyl conformations were done utilizing CNS SA-omit maps holding the protease residue coordinates fixed. Eight possible conformations were sampled, four chair and four boat conformations, including 2-fold disordered inhibitor conformations. A 2-fold boat conformation was found to provide the best fit to the density. During model building and refinement, 5% of the data was reserved for cross validation of the refinement progress. The atomic coordinates have been deposited in the Protein Data Bank (PDB entry 2FLE). The X-ray data collection and refinement statistics are shown in Table 4.

Molecular Modeling. (a). Energy Calculations from the Modeled Complexes with Cha in the Boat and Chair Conformations. The starting point for our calculations was the crystal structures of the HIV-1 PR bound to two ligands: the inhibitor **PC** studied in the present work and the inhibitor **CGP 53820**, from PDB entry 1HII[25] (see Table 1 for chemical structures). In every case, hydrogen atoms were added using the Biopolymer module in InsightII.[40] We chose to have the active site aspartic acid dyad monoprotonated by neutralizing the residue A25. The position of the protons was optimized using an energy minimization protocol with a gradient tolerance of 0.01 kcal/Å^2 in the CHARMM suite of programs.[41] The solvent was modeled by surrounding these complexes by 10 Å layer with about 2000 water molecules by using the module Soak in InsightII.[40] The water molecules were equilibrated by a 0.5 ns molecular dynamics run at 300 K and a NVT ensemble using the CHARMM module with CHARMM potentials available in InsightII. To predict the relative stability of either chair or boat conformations in both systems, we built copies of these complexes with their alternative Cha conformations. In this way, we generated the HIV-1 PR^{V82A}−**PC** complex with the Cha in a chair conformation and a HIV-1 PR−**CGP 58320** complex with the inhibitor Cha side chain in a boat conformation. The Cha fragments were built using their original χ_1 and χ_2 side chain torsion angles found in the crystal structures. All systems were then subject to a two-step molecular mechanics protocol. The first step contained an energy minimization with an ABNR minimizer and a gradient tolerance of 0.01. In the second step, more than 350 ps of dynamics were performed on a subsystem of the complex containing all atoms at a 10 Å radius from the ligand, at 300 K in a NVT ensemble. The affinity of the ligands for the enzyme was gauged using their molecular mechanics-based interaction energy, evaluated in the last 200 ps of the MD production stage.

(b). Energy Evaluation of the Structures Resulting from the X-ray Refinement. The X-ray refinement allows the fitting of the Cha fragment in both boat and retracted chair conformation (see Figure 2). We have used the coordinates of these two structures as the starting point for their energy optimization. The protons were added and optimized as above. Solvation was taken into account by the equilibrated 10 Å layer with about 2000 water molecules described above. At this point, the whole system was energy-minimized to alleviate the clashes resulting from X-ray refinement with a protocol starting with 200 steps of SD minimization followed by an ABNR minimization with a gradient tolerance of 0.05 kcal/Å^2. The affinity of the ligands was evaluated as above.

Acknowledgment. This work was supported by grants from the NIH (NIH Grant AI28571 to B.M.D. and Post-Doctoral Fellowship from Training Grant T32-CA09126 to J.C.C.), the Spanish Ministry of Education and Science (Grant CTQ2006-07854/BQU to F.J.S. and a fellowship to P.G.), and Xunta de Galicia (to F.S. and Grant PGIDT06PXIB209109PR to F.J.S.). We thank the CESGA for computer time.

Supporting Information Available: Results from elemental analysis. This material is available free of charge via the Internet at http://pubs.acs.org.

References

(1) Wlodawer, A.; Erickson, J. W. Structure-based inhibitors of HIV-1 protease. *Annu. Rev. Biochem.* **1993**, *62*, 543–585.

(2) Erickson, J. W.; Burt, S. K. Structural mechanisms of HIV drug resistance. *Annu. Rev. Pharmacol. Toxicol.* **1996**, *36*, 545–571.

(3) Wlodawer, A.; Vondrasek, J. Inhibitors of HIV-1 protease: A major success of structure-assisted drug design. *Annu. Rev. Biophys. Biomol. Struct.* **1998**, *27*, 249–284.

(4) Condra, J. H.; Schleif, W. A.; Blahy, O. M.; Gabryelski, L. J.; Graham, D. J.; Quintero, J. C.; Rhodes, A.; Robbins, H. L.; Roth, E.; Shivaprakash, M.; Titus, D.; Yang, T.; Teppler, H.; Squires, K. E.; Deutsch, P. J.; Emini, E. A. In vivo emergence of HIV-1 variants resistant to multiple protease inhibitors. *Nature* **1998**, *374*, 569–571.

(5) Ho, D. D.; Toyoshima, T.; Mo, H.; Kempf, D. J.; Norbeck, D.; Chen, C.-M.; Wideburg, N. E.; Burt, S. K.; Erickson, J. W.; Singh, M. K. Characterization of human immunodeficiency virus type 1 variants with increased resistance to a C_2-symmetric protease inhibitor. *J. Virol.* **1994**, *68*, 2016–2020.

(6) Ohtaka, H.; Muzammil, S.; Schön, A.; Velazquez-Campoy, A.; Vega, S.; Freire, E. Thermodynamic rules for the design of high affinity HIV-1 protease inhibitors with adaptability to mutations and high selectivity towards unwanted targets. *Int. J. Biochem. Cell Biol.* **2004**, *36*, 1787–1799.

(7) Clemente, J. C.; Moose, R. E.; Hemrajani, R.; Whitford, L. R. S.; Govindasamy, L.; Reutzel, R.; McKenna, R.; Agbandje-McKenna, M.; Goodenow, M. M.; Dunn, B. M. Comparing the accumulation of active- and nonactive-site mutations in the HIV-1 protease. *Biochemistry* **2004**, *43*, 12141–12151.

(8) Baldwin, E. T.; Bhat, T. N.; Liu, B.; Pattabiraman, N.; Erickson, J. W. Structural basis of drug resistance for the V82A mutant of HIV-1 proteinase. *Nat. Struct. Biol.* **1995**, *2*, 244–249.

(9) Matthews, B. W. Studies on protein stability with T4 lysozyme. *Adv. Protein Chem.* **1995**, *46*, 249–278.

(10) Hosur, M. V.; Bhat, T. N.; Kempf, D. J.; Baldwin, E. T.; Liu, B.; Gulnik, S.; Wideburg, N. E.; Norbeck, D. W.; Appelt, K.; Erickson, J. W. Influence of stereochemistry on activity and binding modes for C_2 symmetry-based diol inhibitors of HIV-1 protease. *J. Am. Chem. Soc.* **1994**, *116*, 847–855.

(11) Ohtaka, H.; Freire, E. Adaptive inhibitors of the HIV-1 protease. *Prog. Biophys. Mol. Biol.* **2005**, *88*, 193–208.

(12) Yin, P. D.; Das, D.; Mitsuya, H. Overcoming HIV drug resistance through rational drug design based on molecular, biochemical, and structural profiles of HIV resistance. *Cell. Mol. Life Sci.* **2006**, *63*, 1706–1724.

(13) King, N. M.; Prabu-Jeyabalan, M.; Nalivaika, E. A.; Schiffer, C. A. Combating susceptibility to drug resistance: lessons from HIV-1 protease. *Chem. Biol.* **2004**, *11*, 1333–1338.

(14) Vega, S.; Kang, L.-W.; Velazquez-Campoy, A.; Kiso, Y.; Amzel, L. M.; Freire, E. A structural and thermodynamic escape mechanism from a drug resistant mutation of the HIV-1 protease. *Proteins* **2004**, *55*, 594–602.

(15) Hoppe, D.; Marr, F.; Brüggemann, M. Enantioselective synthesis by lithiation adjacent to oxygen and electrophile incorporation. In *Topics in Organometallic Chemistry*; Hodgson, D. M., Ed.; Springer: Berlín, 2003; Vol. 5, pp. 61–138.

(16) Schwerdtfeger, J.; Hoppe, D. Stereoselective generation of 1-acyloxy-2-amino carbanions by deprotonation; synthesis of enantiomerically and diastereomerically pure β-amino alcohols. *Angew. Chem., Int. Ed.* **1992**, *31*, 1505–1507.

(17) (a) Reetz, M. T.; Drewes, M. W.; Schwickardi, R. Preparation of enantiomerically pure α-*N*,*N*-dibenzylamino aldehydes: *S*-2-(*N*,*N*-dibenzylamino)-3-phenylpropanal. *Org. Synth.* **1999**, *76*, 110–122. (b) Alexander, C. W.; Liotta, D. C. A diastereoselective synthesis of (2*S*,3*R*,4*S*)-2-amino-1-cyclohexyl-6-methylheptane-3,4-diol, the Abbott aminodiol. *Tetrahedron Lett.* **1996**, *37*, 1961–1964.

(18) For the preparation of **3c** and **4c** see: Weber, B.; Kolczewski, S.; Fröhlich, R.; Hoppe, D. Facile and highly stereoselective synthesis of the C_2-symmetrical diamino diol core-unit of HIV-1 protease inhibitors and of their symmetrical and unsymmetrical analogs from lithiated 2-(dibenzylamino)alkyl carbamates: oxidative dimerization. *Synthesis* **1999**, 1593–1606.

(19) van Bebber, J.; Ahrens, H.; Fröhlich, R.; Hoppe, D. Efficient desymmetrization of *meso-cis*-1,2-cyclohexanedimethanol with differentiation between diastereotopic and enantiotopic C−H bonds by (−)-sparteine-mediated deprotonation. *Chem.−Eur. J.* **1999**, *5*, 1905–1916.

(20) For a different preparation of **5c** see: Kempf, D. J.; Sowin, T. J.; Doherty, E. M.; Hannick, S. M.; Codavoci, L.; Henry, R. F.; Green, B. E.; Spanton, S. G.; Norbeck, D. W. Stereocontrolled synthesis of C_2-symmetric and pseudo-C_2-symmetric diamino alcohols and diols for use in HIV protease inhibitors. *J. Org. Chem.* **1992**, *57*, 5692–5700.

(21) The side chain was prepared following the literature procedure: Kempf, D. J.; Codacovi, L.; Wang, X. C.; Kohlbrenner, W. E.; Wideburg, N. E.; Saldivar, A.; Vasavanonda, S.; Marsh, K. C.; Bryant, P.; Sham, H. L.; Green, B. E.; Betebenner, D. A.; Erickson, J.; Norbeck, D. W. Symmetry-based inhibitors of HIV protease. Structure–activity studies of acylated 2,4-diamino-1,5-diphenyl-3-hydroxypentane and 2,5-

diamino-1,6-diphenylhexane-3,4-diol. *J. Med. Chem.* **1993**, *36*, 320–330.
(22) Tie, Y.; Boross, P. I.; Wang, Y.-F.; Gaddis, L.; Hussain, A. K.; Leshchenko, S.; Ghosh, A. K.; Louis, J. M.; Harrison, R. W.; Weber, I. T. High resolution crystal structures of HIV-1 protease with a potent non-peptide inhibitor (UIC-94017) active against multi-drug-resistant clinical strains. *J. Mol. Biol.* **2004**, *338*, 341–352.
(23) Clark, T.; McKervey, M. A. Saturated hydrocarbons. In *Comprehensive Organic Chemistry* 1st ed.; Stoddart, J. F. Ed.; Pergamon Press Ltd.: Oxford, 1979; Vol. 1, pp 59–60.
(24) Lee, T.; Le, V.-D.; Lim, D.; Lin, Y.-C.; Morris, G. M.; Wong, A. L.; Olson, A. J.; Elder, J. H.; Wong, C.-H. Development of a new type of protease inhibitors, efficacious against FIV and HIV variants. *J. Am. Chem. Soc.* **1999**, *121*, 1145–1155.
(25) Priestle, J. P.; Fässler, A.; Rösel, J.; Tintelnot-Blomley, M.; Strop, P.; Grütter, M. G. Comparative analysis of the X-ray structures of HIV-1 and HIV-2 proteases in complex with CGP 53820, a novel pseudosymmetric inhibitor. *Structure* **1995**, *3*, 381–389.
(26) Perola, E.; Charifson, P. S. Conformational analysis of drug like molecules bound to proteins: an extensive study of ligand reorganization upon binding. *J. Med. Chem.* **2004**, *47*, 2499–2510.
(27) Koshland, D. E. Jr. Application of a theory of enzyme specificity to protein synthesis. *Proc. Natl. Acad. Sci. U.S.A.* **1958**, *44*, 98–104.
(28) Bosshard, H. R. Molecular recognition by induced fit: How fit is the concept. *News. Physiol. Sci.* **2001**, *16*, 171–173.
(29) Hintze, F.; Hoppe, D. Enantioselective synthesis of (*S*)-1-methyldodecyl acetate, a pheromone of *Drosophila mulleri*, via (−)-sparteine-assisted deprotonation of 1-dodecanol. *Synthesis* **1992**, 1216–1218.
(30) Schwerdtfeger, J.; Kolczewski, S.; Weber, B.; Fröhlich, R.; Hoppe, D. Stereoselective deprotonation of chiral and achiral 2-aminoalkyl carbamates: Synthesis of optically active β-amino alcohols via 1-oxy-substituted alkyllithium intermediates. *Synthesis* **1999**, 1573–1592.
(31) Ido, E.; Han, H.; Kezdy, F. J.; Tang, J. Kinetic studies of human immunodeficiency virus type 1 protease and its active-site hydrogen bond mutant A28S. *J. Biol. Chem.* **1991**, *266*, 24359–24366.
(32) Goodenow, M. M.; Bloom, G.; Rose, S. L.; Pomeroy, S. M.; O'Brien, P. O.; Perez, E. E.; Sleasman, J. W.; Dunn, B. M. Naturally ocurring amino acid polymorphisms in human immunodeficiency virus type 1 (HIV-1) Gag p7 (NC) and the C-cleavage site impact Gag-Pol processing by HIV-1 protease. *Virology* **2002**, *292*, 137–149.
(33) Wain-Hobson, S.; Sonigo, P.; Danos, O.; Cole, S.; Alizon, M. Nucleotide sequence for the AIDS virus, LAV. *Cell* **1985**, *40*, 9–17.
(34) Clemente, J. C.; Hemrajani, R.; Blum, L. E.; Goodenow, M. M.; Dunn, B. M. Secondary mutations M36I and A71V in the human immunodeficiency virus type 1 protease can provide an advantage for the emergence of the primary mutation D30N. *Biochemistry* **2003**, *42*, 15029–15035.
(35) Dunn, B. M.; Gustchina, A.; Wlodawer, A.; Kay, J. Subsite preferences of retroviral proteinases. *Methods Enzymol.* **1994**, *241*, 254–278.
(36) Bhatt, D.; Dunn, B. M. Chimeric aspartic proteinases and active site binding. *Bioorg. Chem.* **2000**, *28*, 374–393.
(37) Otwinowski, Z.; Minor, W. Processing of X-ray diffraction data collected in oscillation mode. *Methods Enzymol.* **1997**, *276*, 307–326.
(38) Brünger, A. T.; Adams, P. D.; Clore, G. M.; DeLano, W. L.; Gros, P.; Grosse-Kunstleve, R. W.; Jiang, J.-S.; Kuszewski, J.; Nilges, M.; Pannu, N. S.; Read, R. J.; Rice, L. M.; Simonson, T.; Warren, G. L. Crystallography and NMR system: A new software suite for macromolecular structure determination. *Acta Crystallogr., Sect. D: Biol. Crystallogr.* **1998**, *54*, 905–921.
(39) Jones, T. A.; Zou, J.-Y.; Cowan, S. W.; Kjeldgaard, M. Improved methods for building protein models in electron density maps and the location of errors in these models. *Acta Crystallogr., Sect. A: Found. Crystallogr.* **1991**, *47*, 110–119.
(40) *InsightII*, Biopolymer and Soak are trademarks of Accelrys Inc., San Diego, CA.
(41) Brooks, B. R.; Bruccoleri, R. E.; Olafson, B. D.; States, D. J.; Swaminathan, S.; Karplus, M. CHARMM: A program for macromolecular energy, minimization, and dynamics calculations. *J. Comput. Chem.* **1983**, *4*, 187–217.

JM701170F